Published by Institute of Physics Publishing for SISSA

Received: *October 10, 2007*
Accepted: *December 17, 2007*
Published: *January 8, 2008*

Solving the degeneracy of the lepton-flavor mixing angle $\theta_{\rm ATM}$ by the T2KK two detector neutrino oscillation experiment

Kaoru Hagiwara[a] **and Naotoshi Okamura**[ab]

[a] *KEK Theory Division and SOKENDAI, Tsukuba, 305-0801 Japan*
[b] *Yukawa Institute for Theoretical Physics, Kyoto University, Kyoto, 606-8502 Japan*
E-mail: okamura@yukawa.kyoto-u.ac.jp

Abstract: If the atmospheric neutrino oscillation amplitude, $\sin^2 2\theta_{\rm ATM}$ is not maximal, there is a two fold ambiguity in the neutrino parameter space: $\sin^2\theta_{\rm ATM} > 0.5$ or $\sin^2\theta_{\rm ATM} < 0.5$. In this article, we study the impact of this degeneracy, the so-called octant degeneracy, on the T2KK experiment, which is a proposed extension of the T2K (Tokai-to-Kaimoka) neutrino oscillation experiment with an additional water Čerenkov detector placed in Korea. We find that the degeneracy between $\sin^2\theta_{\rm ATM} = 0.40$ and 0.60 can be resolved at the 3σ level for $\sin^2 2\theta_{\rm RCT} > 0.12$ (0.08) for the optimal combination of a 3.0° off-axis beam (OAB) at SK ($L = 295$km) and a 0.5° OAB at $L = 1000$km with a far detector of 100kton volume, after 5 years of exposure with $1.0\ (5.0) \times 10^{21}$POT/year, if the hierarchy is normal. We also study the influence of the octant degeneracy on the capability of T2KK experiment to determine the mass hierarchy and the leptonic CP phase. The capability of rejecting the wrong mass hierarchy grows with increasing $\sin^2\theta_{\rm ATM}$ when the hierarchy is normal, whereas it is rather insensitive to $\sin^2\theta_{\rm ATM}$ for the inverted hierarchy. We also find that the 1σ allowed region of the CP phase is not affected significantly even when the octant degeneracy is not resolved. All our results are obtained for the 22.5 kton Super-Kamiokande as a near detector and without an anti-neutrino beam.

Keywords: Neutrino Physics, Standard Model.

JHEP01(2008)022

Contents

1. Introduction **1**

2. Oscillation formular and experimental bound **3**

3. Analysis method **6**

4. Octant degeneracy and the T2KK experiment **8**

5. Mass hierarchy and the octant degeneracy **13**

6. CP phase and the octant degeneracy **17**

7. Summary **19**

JHEP01(2008)022

1. Introduction

A decade ago, it was difficult to believe that neutrinos have mass and the lepton flavor mixing matrix, the Maki-Nakagawa-Sakata (MNS) matrix [1], has two large mixing angles [2 – 7]. Within the three neutrino framework, 2 mass-squared differences, 3 mixing angles, and 1 CP phase can be resolved by neutrino oscillation experiments. So far, the magnitude of the larger mass-squared difference, the magnitude and the sign of the smaller one, two of the three mixing angles, and the upper bound of the third mixing angle have been known. The sign of the larger mass-squared difference (the mass hierarchy pattern), the magnitude of the third mixing angle ($\theta_{\rm RCT}$), and the leptonic CP phase ($\delta_{\rm MNS}$) are yet to be measured.

In the previous papers [8, 9], we studied in detail the physics impacts of the idea [10] of placing a far detector in Korea along the T2K neutrino beam line. For concreteness we examined the effects of placing a 100kton water Čerenkov detector in Korea, about $L = 1000$km away from J-PARC (Japan Proton Accelerator Research Complex) [11], during the T2K (Tokai-to-Kamioka) experiment period [12], which plans to accumulate 5×10^{21} POT (protons on target) in 5 years. We find that this experiment with two detectors for one beam, which may be called the T2KK experiment [13], can determine the mass hierarchy pattern, by comparing the $\nu_\mu \to \nu_e$ transition probability measured at Super-Kamiokande (SK) and that at a far detector in Korea. Moreover, both the sine and cosine of the CP phase can be measured from the energy dependence of the $\nu_\mu \to \nu_e$ oscillation probability, which can be measured by selecting the quasi-elastic charged current events. By studying these physics merits of the T2KK experiment semi-quantitatively, we find an optimal combination of a 3° off-axis beam (OAB) at SK and a 0.5° OAB in the east

coast of Korea at $L = 1000$km, for which the mass hierarchy and the CP phase ($\delta_{\rm MNS}$) can be determined without invoking an anti-neutrino phase [8, 9], when the mixing angle $\theta_{\rm RCT}$ is not too small. In the related study [14], a grander prospect of the T2KK idea has been explored, where two identical huge detectors of several 100kton volume is placed in Kamioka and in Korea, and the future upgrade of the J-PARC beam intensity has also been considered. The idea of placing two detectors along one neutrino beam has also been explored for the Fermi Lab. neutrino beam [15].

In this report, we focus on the yet another degeneracy in the neutrino parameter space, which shows up when the amplitude of the atmospheric neutrino oscillation, $\sin^2 2\theta_{\rm ATM}$, is not maximal. Hereafter, we call this degeneracy between $\sin^2\theta_{\rm ATM} > 0.5$ and $\sin^2\theta_{\rm ATM} < 0.5$, or between "$90^\circ - \theta_{\rm ATM}$" and "$\theta_{\rm ATM}$", as the octant degeneracy [16]. The main objective of this paper is to study the capability of a T2KK two-detector experiment to resolve this octant degeneracy when the off-axis angles at the near and the far detectors are chosen to optimize the sensitivity to the mass hierarchy, i.e., 3° SK and 0.5° at $L = 1000$km, [8, 9]. We also explain why the octant degeneracy can be resolved efficiently in this particular setting, and how it influences the mass hierarchy determination capability of the experiment.

Since the best fit value of the mixing angle $\theta_{\rm ATM}$ is 45° [2 – 4], we set $\sin^2 2\theta_{\rm ATM} = 1$ in all our previous studies [8, 9], and hence we did not pay attention on physics impacts of the octant degeneracy. However, we are concerned that the octant degeneracy affect the capability of the T2KK experiment for the mass hierarchy determination and the CP phase measurement, because the leading term of the $\nu_\mu \to \nu_e$ oscillation probability is proportional to $\sin^2\theta_{\rm ATM}$, not $\sin^2 2\theta_{\rm ATM}$. If the value of $\sin^2 2\theta_{\rm ATM}$ is 0.99, which is 1% smaller than the maximal mixing, the value of $\sin^2\theta_{\rm ATM}$ is $\sin^2\theta_{\rm ATM} = 0.45$ or 0.55, which differ by 20%.

For $\sin^2 2\theta_{\rm ATM} = 0.92$, which is still allowed at the 90% CL [2 – 4], $\sin^2\theta_{\rm ATM} = 0.64$ or 0.36, which differ by almost a factor of two. Therefore, we also examine impacts of varying $\sin^2\theta_{\rm ATM}$ on the mass hierarchy determination and the CP phase measurement by T2KK. In our semi-quantitatively analysis, we follow the strategy of ref. [8, 9] where we adopt SK as a near side detector and postulate a 100 kton water Čerenkov detector at $L = 1000$km, and the J-PARC neutrino beam orientation is adjusted to 3.0° at SK and 0.5° at the Korean detector site. We study this particular combination of the off-axis angles in detail because it gives the optimal sensitivity to determine the mass hierarchy in Ref [8, 9]. For instance, while the inverted hierarchy cannot be excluded ($\Delta\chi^2 \simeq 3$) with the 2.5° OAB both at SK and Korea, it can be excluded at more than 4σ level ($\Delta\chi^2 \simeq 22$) when we choose 3.0° for SK and 0.5° for Korea. The above results were found when the atmospheric mixing angles are assumed to be maximum ($\sin^2\theta_{\rm ATM} = 0.5$). In this report, we study in detail how non-maximum mixing affects the mass hierarchy determination and if we can resolve the octant degeneracy in this optimal setting of a T2KK experiment.

This article is organized as follows. In section 2, we fix our notation and show how the octant degeneracy affects the oscillation probabilities. In section 3, we review our analysis method and present an explicit form of the $\Delta\chi^2$ function which we use to measure the capability of the T2KK experiment semi-quantitatively. In section 4, we show the results of our numerical calculation on the resolution of the octant degeneracy. In section 5, we

JHEP01(2008)022

examine the capability of the T2KK experiment for the mass hierarchy determination, in the presence of the octant degeneracy. We also show the effect of the octant degeneracy on the CP phase measurement in section 6. In the last section, we summarize our results and give discussions.

2. Oscillation formular and experimental bound

When a neutrino of flavor α is created at the neutrino source with energy E, it is a mixture of the mass eigenstates, ν_i

$$|\nu_\alpha\rangle = \sum_{i=1}^{3} U_{\alpha i} \ |\nu_i\rangle \ , \qquad (\alpha = e, \mu, \tau) \tag{2.1}$$

where $U_{\alpha i}$ is the element of the Maki-Nakagawa-Sakata (MNS) matrix [1]. Without loosing generality, we can take U_{e2} and $U_{\mu 3}$ to be real and non-negative and allow U_{e3} to have a complex phase $\delta_{\rm MNS}$ [17, 18].

After traveling the distance L in the vacuum, a neutrino flavor eigenstate $|\nu_\beta\rangle$ is found with the probability

$$\begin{aligned} P_{\nu_\alpha \to \nu_\beta} &= |\langle \nu_\beta \, | \nu_\alpha(L) \rangle|^2 = \left| \sum_{j=1}^{3} U_{\alpha j} \exp\left(-i \frac{m_j^2}{2E} L \right) U_{\beta j}^* \right|^2 \\ &= \delta_{\alpha\beta} - 4 \sum_{i>j} \Re(U_{\alpha i}^* U_{\beta i} U_{\alpha j} U_{\beta j}^*) \sin^2 \frac{\Delta_{ij}}{2} + 2 \sum_{i>j} \Im(U_{\alpha i}^* U_{\beta i} U_{\alpha j} U_{\beta j}^*) \sin \Delta_{ij} \ , \end{aligned} \tag{2.2}$$

where m_j is the mass of ν_i and Δ_{ij} is

$$\Delta_{ij} \equiv \frac{m_j^2 - m_i^2}{2E} L \simeq 2.534 \frac{\left(m_j^2 - m_i^2 \right) [\mathrm{eV}^2]}{E[\mathrm{GeV}]} L \, [\mathrm{km}] \ . \tag{2.3}$$

Eq. 2.2 shows that neutrino flavor oscillation is governed by the two mass-squared differences and the lepton number conserving combinations of the MNS matrix elements.

We take $|\Delta_{13}| > |\Delta_{12}|$ without loosing generality. Under this parameterization, atmospheric neutrino observation [2] and the accelerator based long baseline (LBL) experiments, K2K [3] and MINOS [4], which measure the ν_μ survival probability, are sensitive to the magnitude of the larger mass-squared difference and $U_{\mu 3}$:

$$1.5 \times 10^{-3} \mathrm{eV}^2 < |m_3^2 - m_1^2| < 3.4 \times 10^{-3} \mathrm{eV}^2 \, , \tag{2.4a}$$

$$\sin^2 2\theta_{\rm ATM} \equiv 4 U_{\mu 3}^2 \left(1 - U_{\mu 3}^2 \right) > 0.92 \, , \tag{2.4b}$$

each at the 90% confidence level. Hereafter, we use $\sin^2 \theta_{\rm ATM}$ instead of the $U_{\mu 3}^2$ for brevity ($\sin^2 \theta_{\rm ATM} \equiv U_{\mu 3}^2 = \sin^2 \theta_{23} \cos^2 \theta_{13}$ [18]).

The reactor experiments, which observe the survival probability of the $\bar{\nu}_e$ at $L \sim 1$km from a reactor, are sensitive to the value of the larger mass-squared difference and the

absolute value of U_{e3}. The CHOOZ experiment [5] reported no reduction of the $\bar{\nu}_e$ flux and find

$$\sin^2 2\theta_{\rm RCT} \equiv 4\,|U_{e3}|^2\left(1-|U_{e3}|^2\right) < (0.20,\ 0.16,\ 0.14)$$
$$\text{for}\quad \left|m_3^2-m_1^2\right| = (2.0,\ 2.5,\ 3.0)\times 10^{-3}\text{eV}^2\,, \tag{2.5}$$

at the 90% confidence level. In the following, we denote $|U_{e3}|^2$ as $\sin^2\theta_{\rm RCT}$ ($\sin^2\theta_{\rm RCT}\equiv|U_{e3}|^2=\sin^2\theta_{13}$ [18]).

The solar neutrino observations [6], and the KamLAND experiment [7], which measure the survival probability of ν_e and $\bar{\nu}_e$, respectively, are sensitive to the smaller mass-squared difference and the value of U_{e2}. The present constraints can be expressed as

$$m_2^2-m_1^2 = (8.0\pm0.3)\times10^{-5}\text{eV}^2\,, \tag{2.6a}$$
$$\sin^2\theta_{\rm SOL} = 0.30\pm0.03\,. \tag{2.6b}$$

The sign of $m_2^2-m_1^2$ is determined by the matter effect in the sun [19, 20]. In these experiments, the order of Δ_{12} is roughly 1 and the terms with Δ_{13} oscillate quickly within the experimental resolution of L/E. After averaging out the contribution from Δ_{13}, and neglecting terms of order $\sin^2\theta_{\rm RCT}$, we obtain the relation;

$$\sin^2 2\theta_{\rm SOL}\equiv 4U_{e1}^2U_{e2}^2 = 4U_{e2}^2(1-U_{e2}^2-\left|U_{e3}^2\right|)\,. \tag{2.7}$$

Here, $\sin^2 2\theta_{\rm SOL}\equiv 4U_{e1}^2U_{e2}^2=\sin^2 2\theta_{12}\cos^4\theta_{13}$ [18]. These simple identification, eqs. (2.4b), (2.5), and (2.7), are found to give a reasonably good description of the present data in dedicated studies [21] of the experimental constraints in the three neutrino model. In this paper, we parameterize the CP phase as [18]

$$\delta_{\rm MNS} = -\arg U_{e3}\,. \tag{2.8}$$

The other elements of the MNS matrix can be obtained form the unitary conditions [17]. This convention allows us to express the MNS matrix directly in terms of the three observed amplitudes.

The probability of the neutrino oscillation, eq. (2.2), is modified by the matter effect [19, 20], because only ν_e and $\bar{\nu}_e$ feel the potential by the extra charged current interactions with the electron inside the matter. This extra potential for ν_e is written as

$$a = 2\sqrt{2}G_F E_\nu n_e \simeq 7.56\times10^{-5}[\text{eV}^2]\left(\frac{\rho}{\text{g/cm}^3}\right)\left(\frac{E_\nu}{\text{GeV}}\right)\,, \tag{2.9}$$

where G_F is the Fermi coupling constant, E_ν is the neutrino energy, n_e is the electron number density, and ρ is the matter density. The extra potential for $\bar{\nu}_e$ has the opposite sign. Because the matter effect is small at low energies and also because the phase factor Δ_{12} is small near the first oscillation maximum, $\Delta_{13}\sim\pi$, we find that an approximation of keeping terms linear in the matter effect and Δ_{12} is useful for analyzing the LBL experiments at sub GeV to a few GeV region [8, 9, 22, 23]:

$$P_{\nu_\mu\to\nu_e} = 2(1+q)\sin^2\theta_{\rm RCT}\,(1+A^e)\sin^2\left(\frac{\Delta_{13}}{2}+B^e\right)\,, \tag{2.10a}$$
$$P_{\nu_\mu\to\nu_\mu} = 1-(1-q^2)\,(1+A^\mu)\sin^2\left(\frac{\Delta_{13}}{2}+B^\mu\right)\,, \tag{2.10b}$$

where

$$\sin^2\theta_{\rm ATM} = \frac{1+q}{2}\,, \tag{2.11}$$

and A^α and B^α are the correction terms to the amplitude and the oscillation phase, respectively. For $\alpha = e$, we find

$$A^e = \frac{aL}{\Delta_{13}E}\cos 2\theta_{\rm RCT} - \frac{\Delta_{12}}{2}\frac{\sin 2\theta_{\rm SOL}}{\sin\theta_{\rm RCT}}\sqrt{\frac{1-q}{1+q}}\sin\delta_{\rm MNS}\,, \tag{2.12a}$$

$$B^e = -\frac{aL}{4E}\cos 2\theta_{\rm RCT} + \frac{\Delta_{12}}{2}\left(\frac{\sin 2\theta_{\rm SOL}}{2\sin\theta_{\rm RCT}}\sqrt{\frac{1-q}{1+q}}\cos\delta_{\rm MNS} - \sin^2\theta_{\rm SOL}\right)\,. \tag{2.12b}$$

The octant degeneracy between "$\theta_{\rm ATM}$" and "$90^\circ - \theta_{\rm ATM}$" corresponds to the degeneracy in the sign of q. When q denotes the true value for the octant degeneracy, $-q$ is its fake value.

Using typical numbers of the parameters from the atmospheric neutrino observation and LBL experiments, eq. (2.4), and those from the solar neutrino observation and the KamLAND experiment, eq. (2.6), the $\nu_\mu \to \nu_e$ transition probability can be expressed as

$$P_{\nu_\mu\to\nu_e} \sim 0.05\,(1+q)\left(\frac{\sin^2 2\theta_{\rm RCT}}{0.10}\right)(1+A^e)\sin^2\left(\frac{\Delta_{13}}{2}+B^e\right)\,. \tag{2.13a}$$

$$A^e \sim 0.37\left(\frac{\pi}{\Delta_{13}}\right)\left(\frac{L}{1000[\mathrm{km}]}\right) - \left[0.29\sqrt{\frac{1-q}{1+q}}\left(\frac{0.10}{\sin^2 2\theta_{\rm RCT}}\right)^{1/2}\sin\delta_{\rm MNS}\right]\frac{|\Delta_{13}|}{\pi}\,, \tag{2.13b}$$

$$B^e \sim -0.29\left(\frac{L}{1000[\mathrm{km}]}\right) + \left[0.15\sqrt{\frac{1-q}{1+q}}\left(\frac{0.10}{\sin^2 2\theta_{\rm RCT}}\right)^{1/2}\cos\delta_{\rm MNS} - 0.015\right]\frac{|\Delta_{13}|}{\pi}\,, \tag{2.13c}$$

around the oscillation maximum, $|\Delta_{13}| \sim \pi$. Since the amplitude is proportional to $\sin^2\theta_{\rm ATM} = (1+q)/2$, we expect that the octant degeneracy can be solved by measuring the $\nu_\mu \to \nu_e$ transition probability, if the value of the $\sin^2 2\theta_{\rm RCT}$ is known precisely. Because the first term of A^e changes sign according to the mass hierarchy pattern, $\Delta_{13} \sim \pi$ for the normal and $\Delta_{13} \sim -\pi$ for the inverted, the amplitude of the transition probability is sensitive to the mass hierarchy pattern. The difference between the two hierarchy cases grows with the baseline length when L/E is fixed at around the oscillation maximum [8, 9]. If there is only one detector at $L \sim O(100)$km, the small difference from the matter effect can be absorbed by the sign of q in the leading term of eq. (2.13a).

The q-dependence in A^e and B^e in eqs. (2.13b) and (2.13c) may seem to affect the measurement of the leptonic CP phase. We find, however, that the q-dependence of the coefficient of the CP phase in the $\nu_\mu \to \nu_e$ transition probability is not strong, because

$$(1+q)\sqrt{\frac{1-q}{1+q}} = \sqrt{1-q^2}\,, \tag{2.14}$$

which is independent of the octant degeneracy. Our numerical studies presented below confirms the validity of the above approximations.

Around the first dip of the ν_μ survival probability $|\Delta_{13}| \sim \pi$, we find

$$A^\mu \sim 0.018 \left(\frac{q}{1-q}\right) \left(\frac{\pi}{\Delta_{13}}\right) \left(\frac{L}{1000[\mathrm{km}]}\right) \left(\frac{\sin^2 2\theta_{\mathrm{RCT}}}{0.10}\right) , \tag{2.15a}$$

$$B^\mu \sim 0.014 \left(\frac{q}{1-q}\right) \left(\frac{L}{1000[\mathrm{km}]}\right) \left(\frac{\sin^2 2\theta_{\mathrm{RCT}}}{0.10}\right) - \left[0.037 - 0.008 \left(\frac{\sin^2 2\theta_{\mathrm{RCT}}}{0.10}\right)^{1/2} \cos\delta_{\mathrm{MNS}}\right] \frac{|\Delta_{13}|}{\pi} . \tag{2.15b}$$

Although the shift in the amplitude A^μ and that in the phase B^μ are both proportional to q, their magnitudes are found to be less than 0.7% and 0.5%, respectively, for $|q| < 0.28$, eq. (2.4b). Our numerical results confirm that the measurement of the $\nu_\mu \to \nu_\mu$ survival probability does not contribute significantly to the resolution of the octant degeneracy. On the other hand the smallness of the deviation from the leading contribution allows us to constrain $|m_3^2 - m_1^2|$ and $\sin^2 2\theta_{\mathrm{ATM}}$ accurately by measuring the $\nu_\mu \to \nu_\mu$ survival probability.

3. Analysis method

In this section, we explain how we treat signals and backgrounds in our numerical analysis, and introduce a χ^2 function which measures the capability of the T2KK experiment semi-quantitatively. We consider a water Čerenkov detector at Korea in this study, because it allows us to distinguish clearly the $e^\pm$ events from $\mu^\pm$ events. The fiducial volume of the detector placed at Korea is assumed 100 kton, which is roughly 5 times larger than that of SK, 22.5 kton, in order to compensate for the longer base-line length. We use only the CCQE events in our analysis, because they allow us to reconstruct the neutrino energy event by event [3]. Since the Fermi-motion of the target nucleon would dominate the uncertainty of the neutrino energy reconstruction, which is about 80 MeV [3], we take the width of the energy bin as $\delta E_\nu = 200\,\mathrm{MeV}$ for $E_\nu > 400\,\mathrm{MeV}$. The signals in the i-th energy bin, $E_\nu^i \equiv (200\mathrm{MeV} \times i) < E_\nu < E_\nu^i + \delta E_\nu$, are then calculated as

$$N_\alpha^i(\nu_\mu) = M N_A \int_{E_\nu^i}^{E_\nu^i + \delta E_\nu} \Phi_{\nu_\mu}(E)\; P_{\nu_\mu \to \nu_\alpha}(E)\; \sigma_\alpha^{\mathrm{QE}}(E)\; dE\,, \tag{3.1}$$

where $P_{\nu_\mu \to \nu_\alpha}$ is the neutrino oscillation probability including the matter effect, M is the detector mass, $N_A = 6.017 \times 10^{23}$ is the Avogadro constant, Φ_{ν_μ} is the ν_μ flux from J-PARC [24], and $\sigma_\alpha^{\mathrm{QE}}$ is the CCQE cross section per nucleon in water [3]. For simplicity, the detection efficiencies of both detectors for both ν_μ and ν_e CCQE events are set at 100%. Although 100% efficiency for ν_e CCQE events is not correct, the same results can be obtained by rescaling the exposure time.

We consider the following background events for the signal of e-like events ($\alpha = e$) and μ-like events ($\alpha = \mu$),

$$N_\alpha^{i,\mathrm{BG}} = N_\alpha^i(\nu_e) + N_{\bar\alpha}^i(\bar\nu_e) + N_{\bar\alpha}^i(\bar\nu_\mu)\,, \qquad (\alpha = e\,, \mu)\,, \tag{3.2}$$

respectively. The three terms correspond to the contribution from the secondary neutrino flux of the ν_μ primary beam, which are calculated as in eq. (3.1) where $\Phi_{\nu_\mu}(E)$ is replaced by $\Phi_{\nu_\beta}(E)$ for $\nu_\beta = \nu_e\,, \bar{\nu}_e\,, \bar{\nu}_\mu$. All the primary as well as secondary fluxes used in our analysis are obtained from the web-site [24]. After summing up these background events, the e-like and μ-like events for the i-th bin are obtained as

$$N_\alpha^i = N_\alpha^i(\nu_\mu) + N_\alpha^{i,\mathrm{BG}}\,, \qquad (\alpha = e\,, \mu)\,, \tag{3.3}$$

respectively.

Our interest is the potential of the T2KK experiment for solving the octant degeneracy and its influence on the resolution of the other degeneracies. In order to quantify its capability, we introduce a χ^2 function,

$$\Delta\chi^2 \equiv \chi^2_{\mathrm{SK}} + \chi^2_{\mathrm{Kr}} + \chi^2_{\mathrm{sys}} + \chi^2_{\mathrm{para}}\,, \tag{3.4}$$

which measures the sensitivity of the experiment on the model parameters. The first two terms, χ^2_{SK} and χ^2_{Kr}, measure the parameter dependence of the fit to the SK and the Korean detector data, respectively,

$$\chi^2_{\mathrm{SK,Kr}} = \sum_i \left\{ \left(\frac{(N_e^i)^{\mathrm{fit}} - (N_e^i)^{\mathrm{input}}}{\sqrt{(N_e^i)^{\mathrm{input}}}} \right)^2 + \left(\frac{(N_\mu^i)^{\mathrm{fit}} - (N_\mu^i)^{\mathrm{input}}}{\sqrt{(N_\mu^i)^{\mathrm{input}}}} \right)^2 \right\}\,, \tag{3.5}$$

where $N^i_{\mu,e}$ is the calculated number of events in the i-th bin, and its square root gives the statistical error. Here the summation is over all bins from 0.4 GeV to 5.0 GeV for N_μ, 0.4 GeV to 1.2 GeV for N_e at SK, and 0.4 GeV to 2.8GeV for N_e at Korea. In this energy region, we can include the second peak contribution in our analysis at Korea. We include the contribution of the μ-like events in order to constrain the absolute value of Δ_{13} strongly in this analysis, because a small error of Δ_{13} dilutes the phase shift B^e [8, 9, 22].

N_i^{fit} is calculated by allowing the model parameters to vary freely and by including the systematic errors. We take into account four types of the systematic errors in this analysis. The first systematic error is for the uncertainty in the matter density, for which we allow 3% overall uncertainty along the baseline, independently for T2K (f_ρ^{SK}) and the Tokai-to-Korea experiment (f_ρ^{Kr}):

$$\rho_i^{\mathrm{fit}} = f_\rho^D\, \rho_i^{\mathrm{input}} \qquad (D = \mathrm{SK},\ \mathrm{Kr})\,. \tag{3.6}$$

The second ones are for the overall normalization of each neutrino flux, for which we assume 3% errors,

$$f_{\nu_\beta} = 1 \pm 0.03\,, \tag{3.7}$$

for $(\nu_\beta = \nu_e,\ \bar{\nu}_e, \nu_\mu,\ \bar{\nu}_\mu)$, which are taken common for T2K and the Tokai-to-Korea experiment. The third ones are for the CCQE cross sections,

$$\left(\sigma_\alpha^{\mathrm{QE}}\right)^{\mathrm{fit}} = f_\alpha^{\mathrm{QE}}\, \left(\sigma_\alpha^{\mathrm{QE}}\right)^{\mathrm{input}}\,, \tag{3.8}$$

where α denotes $\ell \equiv e = \mu$ and $\bar{\ell} \equiv \bar{e} = \bar{\mu}$. Because ν_e and ν_μ CCQE cross sections are expected to be very similar theoretically, we assign a common overall error of 3% for ν_e and ν_μ and an independent 3% error for $\bar{\nu}_e$ and $\bar{\nu}_\mu$ CCQE cross sections. Our results are not sensitive to the error of the CCQE cross section and flux normalizations. When we change the errors from 3% to 10%, we find that the minimum $\Delta\chi^2$ reduces only by a few percent level. This is because these are ample ν_μ CCQE events and the errors of ν_μ and ν_e CCQE cross sections are expected to be correlated strongly. The last one is the uncertainty of the fiducial volume, for which we assign 3% error independently for T2K ($f_{\rm V}^{\rm SK}$) and the Tokai-to-Korea experiment ($f_{\rm V}^{\rm Kr}$). $N_\alpha^{i,\rm fit}$ is then calculated as

$$\left[N_\alpha^{i,\rm fit}(\nu_\beta)\right]_{\text{at SK,Kr}} = f_{\nu_\beta}\, f_\alpha^{\rm QE}\, f_{\rm V}^{\rm SK,Kr}\, N_\alpha^i(\nu_\beta)\,, \tag{3.9}$$

and accordingly, $\chi^2_{\rm sys}$ has four terms;

$$\chi^2_{\rm sys} = \sum_{\beta=e,\bar{e},\mu,\bar{\mu}} \left(\frac{f_{\nu_\beta}-1}{0.03}\right)^2 + \sum_{\alpha=\ell,\bar{\ell}} \left(\frac{f_\alpha^{\rm CCQE}-1}{0.03}\right)^2 + \sum_{D=\text{SK, Kr}} \left\{ \left(\frac{f_\rho^D-1}{0.03}\right)^2 + \left(\frac{f_{\rm V}^D-1}{0.03}\right)^2 \right\}. \tag{3.10}$$

To put them shortly, we account for 4 types of uncertainties which are all assigned 3% errors: the effective matter density along each base line, the normalization of each neutrino flux, the CCQE cross sections for ν_l and $\bar{\nu}_l$, and for the fiducial volume of SK, and that of the Korean detector. In total, our $\Delta\chi^2$ function depends on 16 parameters, the 6 model parameters and the 10 normalization factors.

Finally, $\chi^2_{\rm para}$ accounts for external constraints on the model parameters:

$$\chi^2_{\rm para} = \left(\frac{\left(m_2^2-m_1^2\right)^{\rm fit} - 8.2\times10^{-5}{\rm eV}^2}{0.6\times10^{-5}}\right)^2 + \left(\frac{\sin^2 2\theta_{\rm SOL}^{\rm fit} - 0.83}{0.07}\right)^2 + \left(\frac{\sin^2 2\theta_{\rm RCT}^{\rm fit} - \sin^2 2\theta_{\rm RCT}^{\rm input}}{0.01}\right)^2. \tag{3.11}$$

The first two terms correspond to the present experimental constraints from solar neutrino oscillation and KamLAND summarized in eq. (2.6).[1] In the last term, we assume that the planned future reactor experiments [25] should measure $\sin^2 2\theta_{\rm RCT}$ with the expected uncertainty of 0.01.

4. Octant degeneracy and the T2KK experiment

In this section, we show the potential of the T2KK experiment for solving the octant degeneracy and investigate the role of the far detector and the future reactor experiments. We

[1]The most recent results, eq. (2.6), are slightly different from our inputs. Because our analysis is not sensitive to the difference, we use these values for the sake of keeping the consistency with our previous studies [8, 9].

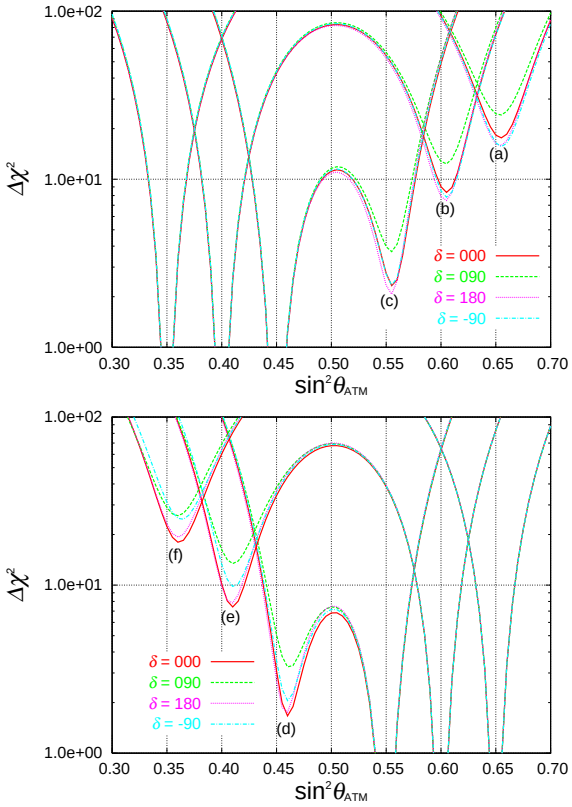

Figure 1: Minimum $\Delta\chi^2$ of the T2KK experiment as a function of $\sin^2\theta_{\rm ATM}$. The event numbers are calculated for a combination of 3.0° OAB at SK and 0.5° OAB at $L = 1000$km with 100 kton water Čerenkov detector, after 5 years running (5×10^{21} POT). The input parameters are chosen as in (4.1). In the left-hand figure, $\sin^2\theta_{\rm ATM}^{\rm input} = 0.35$ (a), 0.40 (b), 0.45 (c) and in the right-hand figure, $\sin^2\theta_{\rm ATM}^{\rm input} = 0.55$ (d), 0.60 (e), 0.65 (f).

show in figure 1 the minimum $\Delta\chi^2$ as a function of $\sin^2\theta_{\rm ATM}$ expected at the T2KK experiment after 5 years of data taking (5×10^{21} POT). The event numbers are calculated for a combination of 3.0° OAB at SK and 0.5° OAB at $L = 1000$km for the following parameters:

$$(m_3^2 - m_1^2)^{\rm input} = 2.5 \times 10^{-3}{\rm eV}^2 \text{ (normal hierarchy)}\,, \tag{4.1a}$$
$$(m_2^2 - m_1^2)^{\rm input} = 8.2 \times 10^{-5}{\rm eV}^2\,, \tag{4.1b}$$
$$\sin^2 2\theta_{\rm RCT}^{\rm input} = 0.10\,, \tag{4.1c}$$
$$\sin^2 2\theta_{\rm SOL}^{\rm input} = 0.83\,, \tag{4.1d}$$
$$\delta_{\rm MNS}^{\rm input} = 0^\circ\,, \pm 90^\circ\,, 180^\circ\,, \tag{4.1e}$$
$$\rho^{\rm input} = 3.0{\rm g/cm}^3 \text{ for } L = 1000{\rm km}\,, \tag{4.1f}$$
$$\rho^{\rm input} = 2.8{\rm g/cm}^3 \text{ for SK}\,. \tag{4.1g}$$

In the left-hand figure of figure 1, we show the cases for the input values $\sin^2\theta_{\rm ATM}^{\rm input}$ =0.35 (a), 0.40 (b), 0.45 (c) and in the right-hand figure, for $\sin^2\theta_{\rm ATM}^{\rm input}$ =0.55 (d), 0.60 (e), 0.65 (f). In each cases, the fit has been performed by surveying the whole parameter space. We find from figure 1, that the octant degeneracy can be solved by T2KK experiment when

JHEP01(2008)022

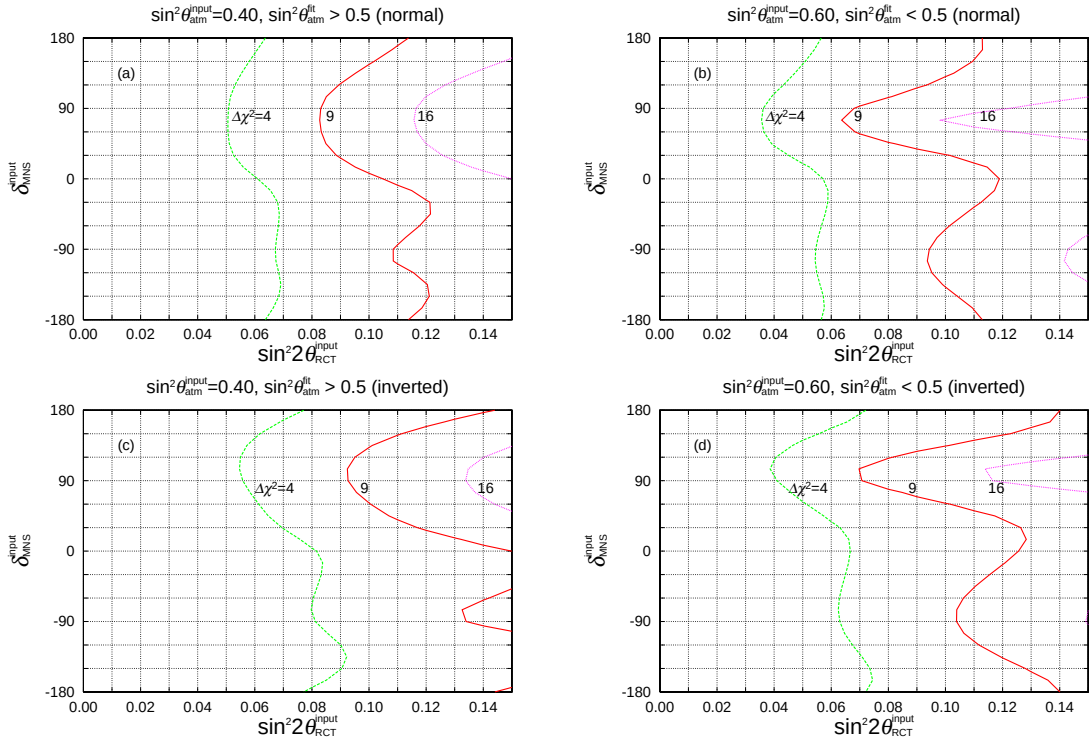

Figure 2: The potential of the T2KK experiment to solve the octant degeneracy with the same OAB combination of the figure 1. In each figures, the event numbers are obtained for the model parameters at various $\sin^2 2\theta^{\rm input}_{\rm RCT}$, $\delta^{\rm input}_{\rm MNS}$ and $\sin^2\theta^{\rm input}_{\rm ATM} = 0.40$ for (a,c), or $\sin^2\theta^{\rm input}_{\rm ATM} = 0.60$ for (b,d), with the normal (a,b) or the inverted (c,d) hierarchy. The other input parameters are same as those of figure 1. All the parameters are taken freely in the fit under the constraint $\sin^2\theta^{\rm fit}_{\rm ATM} > 0.50$ (a,c), or $\sin^2\theta^{\rm fit}_{\rm ATM} < 0.50$ (b,d). The resulting values of minimum $\Delta\chi^2$ are shown as contours for $\Delta\chi^2$ =4, 9, 16.

$\sin^2 2\theta_{\rm ATM} = 0.91$ i.e., between $\sin^2\theta_{\rm ATM} = 0.35$ and 0.65 at 4σ. For $\sin^2 2\theta_{\rm ATM} = 0.96$ the degeneracy between $\sin^2\theta_{\rm ATM} = 0.40$ and 0.60 can be resolved with $\Delta\chi^2 \geq 7$, or at 2.6σ. However, it is difficult to solve the octant degeneracy for $\sin^2 2\theta_{\rm ATM} = 0.99$, between $\sin^2\theta_{\rm ATM} = 0.45$ and 0.55.

In the left-hand figure of figure 1, the minimum $\Delta\chi^2$ for $\delta = 90^\circ$ is larger than those for the other CP phases. In the right-hand figure, the minimum $\Delta\chi^2$ is also largest at $\delta = 90^\circ$. There, however, the minimum $\Delta\chi^2$ for $\delta = -90^\circ$ is slightly larger than those for $\delta = 0^\circ, 180^\circ$.

In order to explore the $\delta_{\rm MNS}$ dependence of the capability of the T2KK experiment to solve the octant degeneracy, we show in figure 2 contours of the minimum $\Delta\chi^2$ in the whole space of $\sin^2 2\theta^{\rm input}_{\rm RCT}$ and $\delta^{\rm input}_{\rm MNS}$. The event numbers are calculated for various $\sin^2 2\theta^{\rm input}_{\rm RCT}$ and $\delta^{\rm input}_{\rm MNS}$ values in each figure, with $\sin^2\theta^{\rm input}_{\rm ATM} = 0.40$ for (a) and (c), or $\sin^2\theta^{\rm input}_{\rm ATM} = 0.60$ for (b) and (d). The other model parameters are set as in eq. (4.1). Figures 2 (a) and (b) are for the normal hierarchy, $m_3^2 - m_1^2 = 2.5 \times 10^{-3}{\rm eV}^2$, and figures 2 (c) and (d) are for the inverted hierarchy, $m_3^2 - m_1^2 = -2.5 \times 10^{-3}{\rm eV}^2$. In performing the fit, all the 16 parameters (6 model parameters and 10 normalization factors) are varied freely under

JHEP01(2008)022

the following constraints: $\sin^2\theta_{\rm ATM}^{\rm fit} > 0.5$ for (a) and (c), $\sin^2\theta_{\rm ATM}^{\rm fit} < 0.5$ for (b) and (d), $(m_3^2-m_1^2)^{\rm fit} > 0$ for (a) and (b), $(m_3^2-m_1^2)^{\rm fit} < 0$ for (c) and (d). From figures 2(a) and 2(c), we find that $\sin^2\theta_{\rm ATM}^{\rm input} = 0.40$ can be distinguished from $\sin^2\theta_{\rm ATM}^{\rm fit} > 0.5$ at $\Delta\chi^2 > 9$ (4) for $\sin^2 2\theta_{\rm RCT}^{\rm input} \gtrsim 0.12$ (0.09) when the normal (inverted) hierarchy is realized. figures 2(b) and 2(d) show that the octant degeneracy can be solved at $\Delta\chi^2 > 9$ for $\sin^2 2\theta_{\rm RCT}^{\rm input} \gtrsim 0.12$ (0.14) when $\sin^2\theta_{\rm ATM}^{\rm input} = 0.60$ for the normal (inverted) hierarchy.

It is found in figures 2(a) and 2(b) that the minimum $\Delta\chi^2$ is highest around $\delta_{\rm MNS}^{\rm input} = 90^\circ$ confirming the trend observed in figure 1. We find from figures 2(c) and 2(d) that the same trend holds even when the neutrino mass hierarchy is inverted. In all the four plots of figure 2, we recognize a high plateau around $\delta_{\rm MNS}^{\rm input} = 90^\circ$ and a lower plateau around $\delta_{\rm MNS}^{\rm input} = -90^\circ$. We can understand the trend by using the approximate expression of the $\nu_\mu \to \nu_e$ transition probability, eq. (2.13). We first note that the $\nu_\mu \to \nu_e$ oscillation probability is proportional to $(1+q)(1+A^e)\sin^2 2\theta_{\rm RCT}$ around the oscillation maxima, $|\Delta_{13} = (2n+1)\pi|$, When $q = -0.2$, the ν_e appearance rate is proportional to $0.8(1+A^e)$. In order to reproduce the same rate for $q = 0.2$, we should find a parameter set that makes the factor $1+A^e$ 40% smaller than its input value, up to the uncertainty in $\sin^2 2\theta_{\rm RCT}$, which is assumed to be $0.01/\sin^2 2\theta_{\rm RCT}^{\rm input}$ in eq. (3.11). This cannot be achieved for $\delta_{\rm MNS}^{\rm input} = 90^\circ$, because the input value of $1+A^e$ takes its minimum value. On the other hand, if $\delta_{\rm MNS}^{\rm input} = -90^\circ$ the input value of $1+A^e$ is large and it can be reduced significantly by choosing $\delta_{\rm MNS}^{\rm fit} = 90^\circ$ in the fit. This explains why the minimum $\Delta\chi^2$ is larger around $\delta_{\rm MNS}^{\rm input} = 90^\circ$ than that around $\delta_{\rm MNS}^{\rm input} = -90^\circ$ when $\sin^2\theta_{\rm ATM} = 0.4$ in figures 2(a) and 2(c). When $q = 0.2$, the same argument tells that we cannot compensate for the large input value of $(1+q)(1+A^e)$ for $\delta_{\rm MNS}^{\rm input} = -90^\circ$. This indeed explains the lower plateau around $\delta_{\rm MNS}^{\rm input} = -90^\circ$ observed in 2(b) and 2(d). The cause of the higher plateau around $\delta_{\rm MNS}^{\rm input} = 90^\circ$ in these figures for $\sin^2\theta_{\rm ATM} = 0.6$ is more subtle. When $\delta_{\rm MNS}^{\rm input} = 90^\circ$, $(1+A^e)^{\rm input}$ takes its smallest value, and the reduction in $(1+q)$ from $(1+q)^{\rm input} = 1+0.2$ to $(1+q)^{\rm fit} = 1-0.2$ can be compensated for by making $(1+A^e)^{\rm fit}$ larger by choosing $\delta_{\rm MNS}^{\rm fit} \simeq -90^\circ$. This, however, necessarily makes the coefficient of $|\Delta_{13}|/\pi$ in eq. (2.13b) have the wrong sign, and hence the ratio of the first peak ($|\Delta_{13}| \sim \pi$) and the second peak ($|\Delta_{13}| \sim 3\pi$) cannot be reproduced. The higher plateau around $\delta_{\rm MNS}^{\rm input} = 90^\circ$ in figures 2(b) and 2(d) for $\sin^2\theta_{\rm ATM}^{\rm input} = 0.6$, and the lower plateau around $\delta_{\rm MNS}^{\rm input} = -90^\circ$ in figures 2(a) and 2(c) for $\sin^2\theta_{\rm ATM}^{\rm input} = 0.4$ can be explained as above.

We show in figure 3 the allowed region of $\sin^2\theta_{\rm ATM}$ and $\sin^2 2\theta_{\rm RCT}$ by the T2KK experiment. The event numbers are generated at $\delta_{\rm MNS}^{\rm input} = 0^\circ$ and $\sin^2 2\theta_{\rm RCT}^{\rm input} = 0.10$ for $\sin^2\theta_{\rm ATM}^{\rm input} = 0.35$, 0.40, 0.45, 0.50, 0.55, 0.60, 0.65 from the 1st to the 7th row. The other input parameters are the same as in eq. (4.1). The allowed regions in the plane of $\sin^2\theta_{\rm ATM}$ and $\sin^2 2\theta_{\rm RCT}$ are shown by the $\Delta\chi^2 = 1$, 4, 9 contours depicted as solid, dashed, and dotted lines, respectively. In the left-hand-side plots, (a), the constraint on $\sin^2 2\theta_{\rm RCT}$ from the future reactor experiment is kept in the $\Delta\chi^2$ function. On the other hand, in the right-hand-side plots, (b), the external constraint on $\sin^2 2\theta_{\rm RCT}$ is removed from the $\Delta\chi^2$ function in eq. (3.11). Comparing figures 3(a) and 3(b), we find that the mirror solution

JHEP01(2008)022

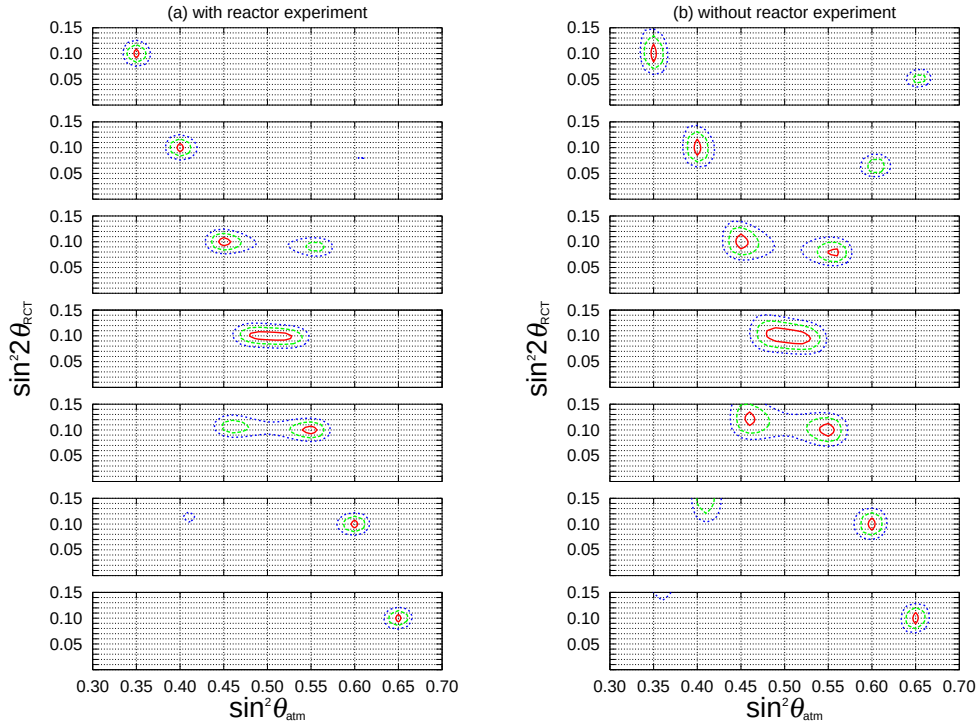

Figure 3: The capability of the T2KK experiment for constraining the $\sin^2\theta_{\rm ATM}$ and $\sin^2 2\theta_{\rm RCT}$. Allowed regions in the plane of $\sin^2\theta_{\rm ATM}$ and $\sin^2 2\theta_{\rm RCT}$ are shown for the same T2KK set up figure 1. In each figure, the event numbers are generated at $\delta_{\rm MNS}^{\rm input} = 0°$ and $\sin^2 2\theta_{\rm RCT}^{\rm input} = 0.10$, for $\sin^2\theta_{\rm ATM}^{\rm input} = 0.35$, 0.40, 0.45, 0.50, 0.55, 0.60, 0.65 from the 1st to the 7th row. The other input parameters are the same as in figure 1. In the left-hand-side plots, (a), we keep the constraint on $\sin^2 2\theta_{\rm RCT}$ form the future reactor experiment, whereas in the right-hand-side plots, (b), we remove the external constraint on $\sin^2 2\theta_{\rm RCT}$ in eq. (3.11). The $\Delta\chi^2 = 1$, 4, 9 contours are shown by the solid, dashed, and dotted lines, respectively.

around

$$\sin^2 2\theta_{\rm RCT}^{\rm fit} = \frac{1+q}{1-q}\sin^2 2\theta_{\rm RCT}^{\rm input} \tag{4.2}$$

cannot be excluded without the information from the future reactor experiment.

Before closing the section, we examine the impact of upgrading the J-PARC beam intensity be a factor of 5 [26] on the resolution of the octant degeneracy. Such an upgrade is desirable especially if the neutrino mass hierarchy is inverted, because the octant degeneracy between $\sin^2\theta_{\rm ATM} = 0.4$ and 0.6 cannot be resolved at 3σ unless $\delta_{\rm MNS} \simeq 90°$; see figures 2(c) and 2(d).

We show in figure 4 the same contour plots as in figure 2, but with 5 times larger exposure (25×10^{21} POT). It is found that the degeneracy between $\sin^2\theta_{\rm ATM} = 0.4$ and 0.6 can now be resolved at 3σ level for $\sin^2 2\theta_{\rm RCT} > 0.08(0.09)$, when the hierarchy is normal (inverted). Comparing figure 2 and figure 4, however, we find that the sensitivity does not improved as much as we would hope with 5 times higher statistics. The minimum $\Delta\chi^2$ value does not grow by a factor 5, because the capability of resolving the octant degeneracy

JHEP01(2008)022

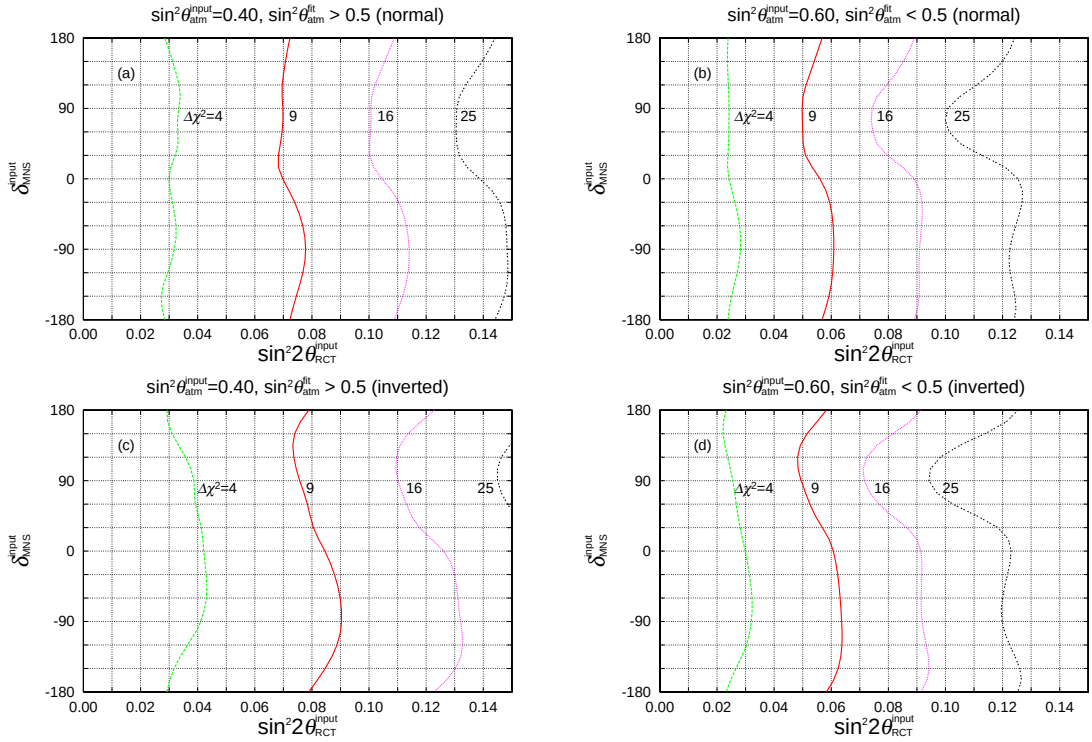

Figure 4: The same as figure 2, but with 5 times larger exposure (25×10^{21} POT).

is now dictated by the accuracy of the external constraint on $\sin^2 2\theta_{\rm RCT}$ from the future reactor experiment,

$$\frac{\delta \sin^2 2\theta_{\rm RCT}}{\sin^2 2\theta_{\rm RCT}} = \frac{0.01}{\sin^2 2\theta_{\rm RCT}}\,, \tag{4.3}$$

which we assume in eq. (3.11). The fractional uncertainty of $\sin^2 2\theta_{\rm RCT}$ is 10% for $\sin^2 2\theta_{\rm RCT} = 0.1$, but it is 17% for $\sin^2 2\theta_{\rm RCT} = 0.06$. If $\sin^2 2\theta_{\rm RCT}$ turns out to be even smaller, the fractional error grows and the mirror solution eq. (4.2) can no more be resolved. If $\sin^2 2\theta_{\rm RCT}$ turns out to be smaller than 0.06, further reduction of its error in the future experiments with reactor and/or the beta beam [27].

5. Mass hierarchy and the octant degeneracy

In this section, we examine the effect of the octant degeneracy on the capability of the T2KK experiment to determine the neutrino mass hierarchy pattern.

Figure 5 shows the minimum $\Delta\chi^2$ as a function of $\sin^2\theta_{\rm ATM}^{\rm input}$ for the T2KK experiment to determine the mass hierarchy pattern with the same OAB combination of figure 1. In each figure, the event numbers are calculated for $\delta_{\rm MNS}^{\rm input} = 0°$ (a), 90° (b), 180° (c), and −90° (d), when the normal hierarchy is realized. The other parameters are listed in eq. (4.1). The fit has been performed by surveying the whole parameter space by assuming the wrong hierarchy. The solid line gives the minimum $\Delta\chi^2$. The open circle denotes the minimum

JHEP01(2008)022

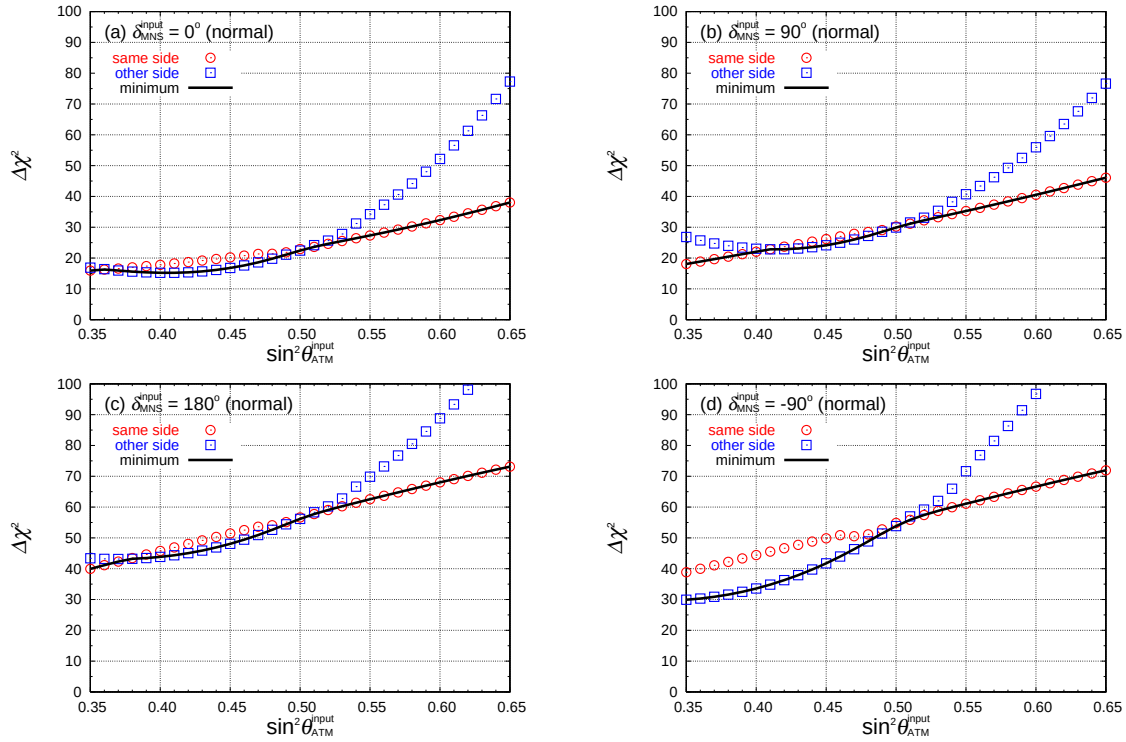

Figure 5: Minimum $\Delta\chi^2$ as a function of $\sin^2\theta_{\rm ATM}^{\rm input}$ for the same T2KK setting as in figure 1. In each figure, the event numbers are calculated for the parameters of eq. (4.1) with $\delta_{\rm MNS}^{\rm input} = 0°$ (a), 90° (b), 180° (c), −90° (d), under the normal hierarchy, and the fit has been performed by assuming the inverted hierarchy. The solid line gives the minimum $\Delta\chi^2$. The open circle (square) denotes the minimum value of $\Delta\chi^2$ when the sign of $q^{\rm input}q^{\rm fit}$ is positive (negative).

$\Delta\chi^2$ when the sign of $q^{\rm input}q^{\rm fit}$, or that of $(1-2\sin^2\theta_{\rm ATM}^{\rm input})(1-2\sin^2\theta_{\rm ATM}^{\rm fit})$, is positive, whereas the open square gives the minimum $\Delta\chi^2$ when $q^{\rm input}q^{\rm fit}$ is negative.

When $q^{\rm fit}$ takes the same sign as $q^{\rm input}$, $\sin^2\theta_{\rm ATM}^{\rm fit} \sim \sin^2\theta_{\rm ATM}^{\rm input}$ is favored, and the reduction of the $\nu_\mu \to \nu_e$ oscillation amplitude $(1+A^e)$ in eq. (2.13b) for the inverted hierarchy, $\Delta_{13} \sim -\pi$, cannot be compensated for in the two detector experiment [8, 9]. Because the $\nu_\mu \to \nu_e$ rate is proportional to $\sin^2\theta_{\rm ATM}^{\rm input}$, the resulting increase in the discrepancy leads to the linear dependence of the minimum $\Delta\chi^2$ on $\sin^2\theta_{\rm ATM}^{\rm input}$ observed for the open circle points. On the other hand, when $\sin^2\theta_{\rm ATM}^{\rm input} < 0.5$ ($q^{\rm input} < 0$), it is possible to compensate for the reduction of the $1+A^e$ factor of the $\nu_\mu \to \nu_e$ oscillation amplitude by choosing $q^{\rm fit} \sim -q^{\rm input}$, since $\sin^2\theta_{\rm ATM}^{\rm fit} = \sin^2\theta_{\rm ATM}^{\rm input}(1+q^{\rm fit})/(1+q^{\rm input}) > 0.5$. This explains why the open square points for $q^{\rm input}q^{\rm fit} < 0$ gives the lowest $\Delta\chi^2$ for $\sin^2\theta_{\rm ATM}^{\rm input} < 0.5$. When $\sin^2\theta_{\rm ATM}^{\rm input}$ is significantly lower than 0.5, however, the enlargement factor of $\sin^2\theta_{\rm ATM}^{\rm fit}/\sin^2\theta_{\rm ATM}^{\rm input} = (1+q^{\rm fit})/(1+q^{\rm input})$ overshoots the reduction due to the matter effect, especially for the $\nu_\mu \to \nu_e$ rate at SK when the matter effect is small. When $\delta_{\rm MNS}^{\rm input} = -90°$, shown in figure 5(d), this reduction in the minimum $\Delta\chi^2$ by using the octant degeneracy is most significant because the overshooting of the $\nu_\mu \to \nu_e$ rate can be partially compensated by choosing $\sin\delta_{\rm MNS}^{\rm fit} > 0$.

JHEP01(2008)022

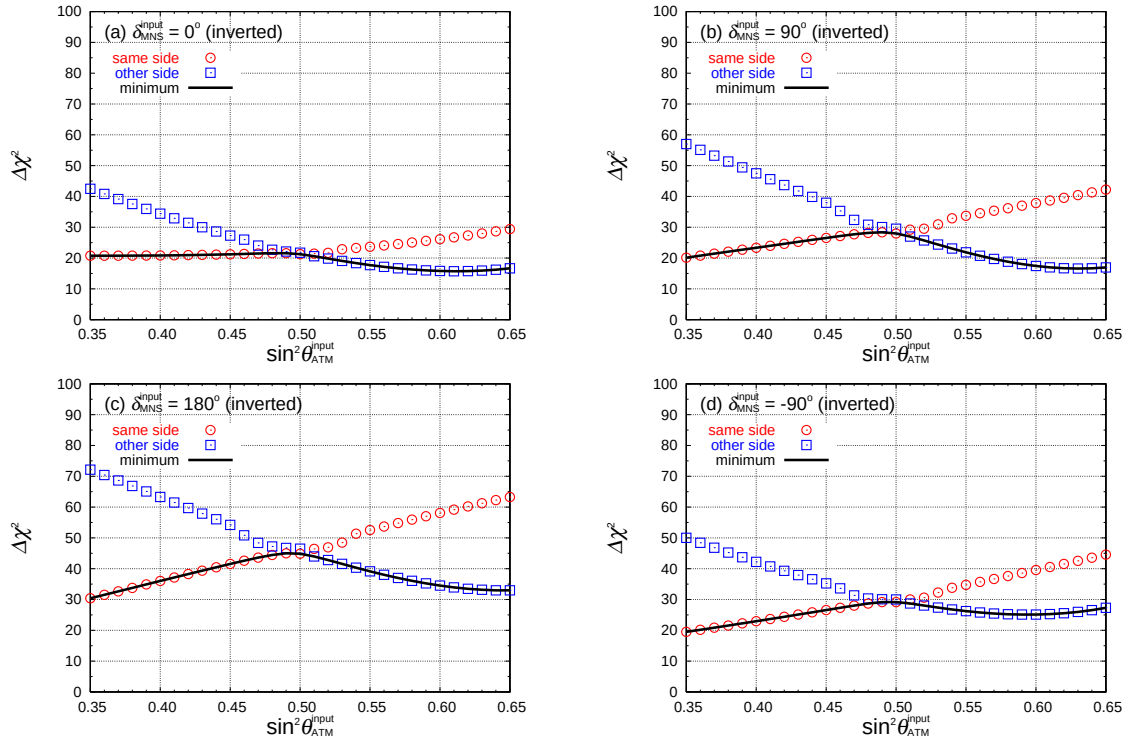

Figure 6: The same as figure 5, but when the inverted hierarchy is realized in nature and the fit is performed by assuming the normal hierarchy.

In figure 6, we show the minimum $\Delta\chi^2$ as a function of $\sin^2\theta^{\rm input}_{\rm ATM}$ when the neutrino mass hierarchy is inverted. The gradual increase of the $\Delta\chi^2$ as $\sin^2\theta^{\rm input}_{\rm ATM}$ grows can also be seen for the open circle points where the fit is restricted to the parameter space that satisfies $q^{\rm fit}q^{\rm input} > 0$. This reflects the increase of the $\nu_\mu \to \nu_e$ event rate as $\sin^2\theta^{\rm input}_{\rm ATM}$ increases, independent of the hierarchy pattern. On the other hand, the minimum $\Delta\chi^2$ for the parameter space of $q^{\rm fit}q^{\rm input} < 0$, plotted by open squares, gives the lowest $\Delta\chi^2$ when $\sin^2\theta^{\rm input}_{\rm ATM} > 0.5$. This is because the reduction of the $\nu_\mu \to \nu_e$ rate in the fit, which is proportional to $\sin^2\theta^{\rm fit}_{\rm ATM}/\sin^2\theta^{\rm input}_{\rm ATM} = (1+q^{\rm fit})/(1+q^{\rm input}) < 1$, for $q^{\rm fit} < 0 < q^{\rm input}$, can compensate for the reduction due to the matter effect when the hierarchy is inverted. The reduction of the minimum $\Delta\chi^2$ due to the octant degeneracy is strong at $\sin^2\theta^{\rm input}_{\rm ATM} > 0.5$ for the inverted hierarchy, and the increased sensitivity to the mass hierarchy pattern for large $\sin^2\theta_{\rm ATM}$ is lost when it is inverted.

In figure 7, we show the capability of the T2KK experiment to determine the mass hierarchy pattern as contour plots of the minimum $\Delta\chi^2$ value on the parameter space of $\sin^2 2\theta^{\rm input}_{\rm RCT}$ and $\delta^{\rm input}_{\rm MNS}$. In each figure, the input date are calculated for the model parameters at various $\sin^2 2\theta^{\rm input}_{\rm RCT}$ and $\delta^{\rm input}_{\rm MNS}$ values, with $\sin^2\theta^{\rm input}_{\rm ATM} = 0.40$ in (a1, b1), $\sin^2\theta^{\rm input}_{\rm ATM} = 0.50$ in (a2, b2), or $\sin^2\theta^{\rm input}_{\rm ATM} = 0.60$ in (a3, b3). The left-hand figures (a1, a2, a3) are for the the normal hierarchy, and the right-hand figures (b1, b2, b3) are for the the inverted hierarchy. The other input parameters are the same as those of figure 5, and in eq. (4.1). All the fit parameters are varied freely to minimize the $\Delta\chi^2$ function, under the constraint of the

JHEP01(2008)022

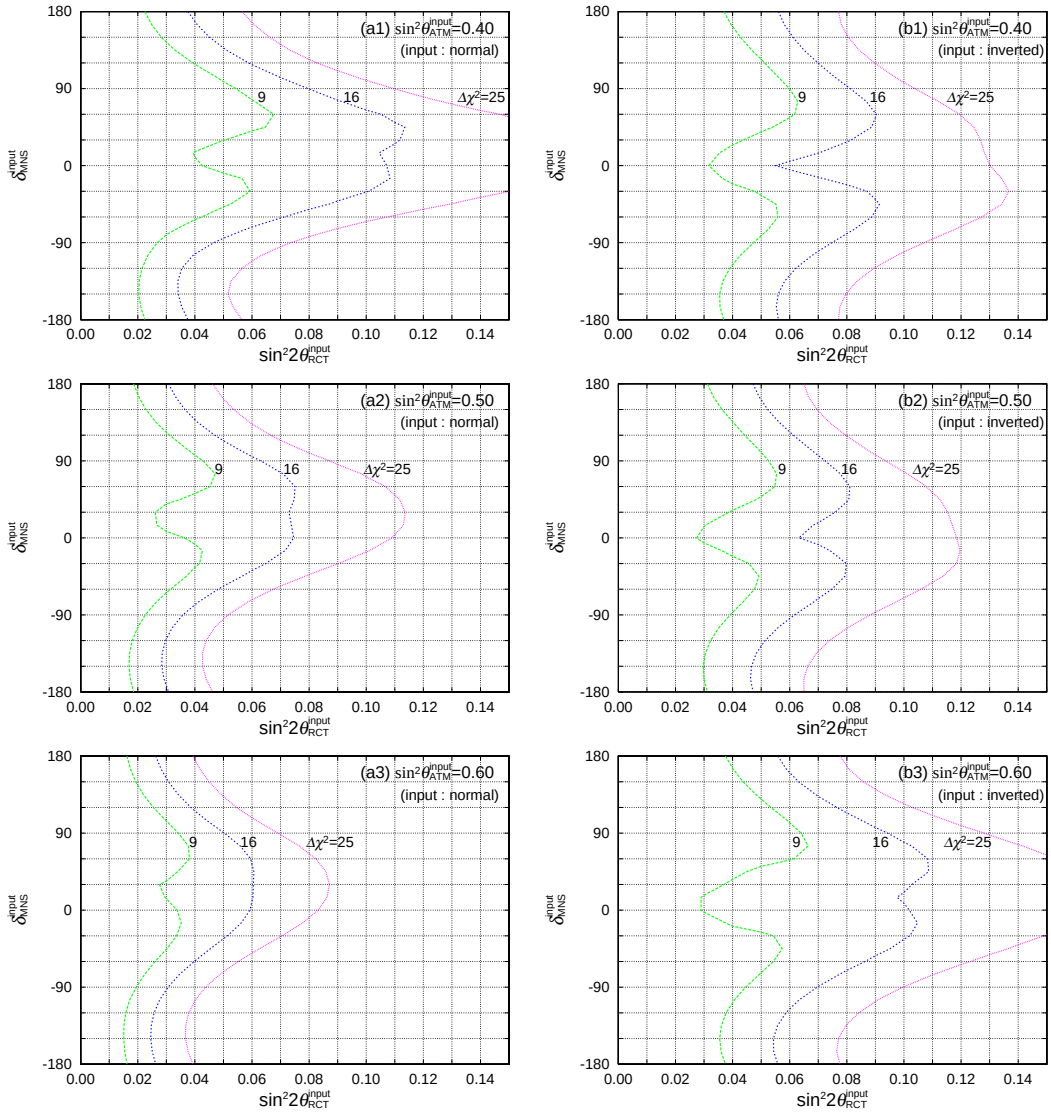

Figure 7: The potential of the T2KK experiment to determine the neutrino mass hierarchy. The input data calculated for the normal hierarchy (a1, a2, a3) or for the inverted hierarchy (b1, b2, b3), and the fit has been performed by assuming the wrong hierarchy. In each figure, the minimum $\Delta\chi^2$ is obtained for the input data calculated at various ($\sin^2 2\theta^{\rm input}_{\rm RCT}$, $\delta^{\rm input}_{\rm MNS}$) with $\sin^2\theta^{\rm input}_{\rm ATM} = 0.40$ for (a1, b1), $\sin^2\theta^{\rm input}_{\rm ATM} = 0.50$ for (a2, b2), or $\sin^2\theta^{\rm input}_{\rm ATM} = 0.60$ for (a3, b3). The other input parameters are the same as those of figure 1. The contours of the minimum $\Delta\chi^2$ are shown for $\Delta\chi^2 = 9$, 16, 25.

opposite mass hierarchy. The resulting values of minimum $\Delta\chi^2$ are shown as contours for $\Delta\chi^2 = 9$, 16, 25. The contours of figures 7(a2) and 7(b2) are identical to those of figure 6 of ref. [9], which we copy for the purpose of comparison.

It is clearly seen in figure 7 that the main feature of the T2KK ability for the mass hierarchy determination at $\sin^2 2\theta^{\rm input}_{\rm ATM} = 0.96$, $\sin^2\theta_{\rm ATM} = 0.4$ (a1, b1) or 0.6 (a3, b3), are not much different from those at $\sin^2 2\theta^{\rm input}_{\rm ATM} = 1.0$ (a2, b2), such as the fact the minimum

JHEP01(2008)022

$\Delta\chi^2$ around $\delta^{\rm input}_{\rm MNS} \simeq 0^\circ$ is smaller than that around $\delta^{\rm input}_{\rm MNS} \simeq 180^\circ$. Close examination of figure 7, however, reveals the followings. In case of the normal hierarchy, $m^2_3 - m^2_1 > 0$, the minimum $\Delta\chi^2$ grows with growing $\sin^2\theta^{\rm input}_{\rm ATM}$, and the mass hierarchy can be determined at 3σ level for $\sin^2 2\theta^{\rm input}_{\rm RCT} \gtrsim 0.07$ if $\sin^2\theta^{\rm input}_{\rm ATM} = 0.40$ (a1), whereas the same holds for $\sin^2 2\theta^{\rm input}_{\rm RCT} \gtrsim 0.04$ if $\sin^2\theta^{\rm input}_{\rm ATM} = 0.60$ (a3). This is mainly because the $\nu_\mu \to \nu_e$ event rate grows with $\sin^2\theta^{\rm input}_{\rm ATM}$ and because the presence of the octant degeneracy does not disturb the measurement significantly, as can be seen from the open circle points in figure 5. In contract, no significant improvement in the hierarchy discrimination power is found for $\sin^2\theta^{\rm input}_{\rm ATM} > 0.5$ in case of the inverted hierarchy. This is because the octant degeneracy between $\sin^2\theta^{\rm fit}_{\rm ATM} = 0.6$ and $\sin^2\theta^{\rm fit}_{\rm ATM} = 0.4$ allows us to compensate for the matter effect reduction of the $\nu_\mu \to \nu_e$ rate. We find that the best hierarchy discrimination is achieved at $\sin^2\theta^{\rm input}_{\rm ATM} = 0.5$ for all $\delta_{\rm MNS}$ values, confirming the trends of figure 6.

Summing up, the T2KK two detector experiments can resolve the mass hierarchy pattern in the presence of the octant degeneracy. If the hierarchy is normal, the discriminating power grows with increasing $\sin^2\theta^{\rm input}_{\rm ATM}$. On the other hand, if the hierarchy is inverted, the discriminating power reduces both at $\sin^2\theta^{\rm input}_{\rm ATM} < 0.5$ and at $\sin^2\theta^{\rm input}_{\rm ATM} > 0.5$: it reduces at $\sin^2\theta_{\rm ATM} < 0.5$ because of the lower rate of the $\nu_\mu \to \nu_e$ events, while it reduces at $\sin^2\theta_{\rm ATM} > 0.5$ because of the octant degeneracy.

6. CP phase and the octant degeneracy

In this section, we investigate the relation between the CP phase measurement and the octant degeneracy.

Figure 8 shows the potential of the T2KK experiment for measuring $\sin^2 2\theta_{\rm RCT}$ and $\delta_{\rm MNS}$ when $\sin^2\theta^{\rm input}_{\rm ATM} = 0.40$ and the hierarchy is normal, $m^2_3 - m^2_1 > 0$. The input values of $\sin^2 2\theta_{\rm RCT}$ and $\delta_{\rm MNS}$ are denoted by solid blobs in each figure, and the 1σ, 2σ, and 3σ allowed regions are shown by solid, dashed, and dotted lines, respectively. The thick contours are for $\sin^2 2\theta^{\rm input}_{\rm RCT} = 0.10$, and the thin contours are for $\sin^2 2\theta^{\rm input}_{\rm RCT} = 0.06$. $\delta^{\rm input}_{\rm MNS} = 0^\circ$ in figure 8(a), 90° in (b), 180° in (c), and -90° in (d). There is no additional allowed region within 3σ when the inverted hierarchy is assumed in the fit, in accordance with figure 7(a1).

When we compare the contours of figure 8 with the corresponding ones in figure 8 of ref. [9] for $\sin^2\theta^{\rm input}_{\rm ATM} = 0.5$, we can clearly identify the islands due to the octant degeneracy. When $\sin^2 2\theta^{\rm input}_{\rm RCT} = 0.10$, the thick contours shows no island at $\delta^{\rm input}_{\rm MNS} = 90^\circ$, but 3σ islands appear at all the other $\delta^{\rm input}_{\rm MNS}$ cases, which is consistent with the result of figure 2(a). In case of $\sin^2\theta^{\rm input}_{\rm RCT} = 0.06$, the contours have 3σ islands for all $\delta^{\rm input}_{\rm MNS}$ cases and a clear 2σ island at $\delta^{\rm input}_{\rm MNS} = -90^\circ$, again consistent with figure 2(a). Close examination of the location of the islands reveals that their center is at around $\sin^2 2\theta^{\rm fit}_{\rm RCT} = \sin^2 2\theta^{\rm input}_{\rm RCT}$ $(0.4)/(0.6)$, as expected by eq. (4.2). The existence of the islands due to the octant degeneracy hence reduces our capability of measuring $\sin^2 2\theta_{\rm RCT}$ significantly.

It is remarkable that the octant degeneracy does not jeopardize the T2KK capability of determining the CP phase, $\delta_{\rm MNS}$: the islands in figure 8 have the $\delta_{\rm MNS}$ values consistent with its input values. This is because the coefficients of both $\sin\delta_{\rm MNS}$ and $\cos\delta_{\rm MNS}$ in the $\nu_\mu \to \nu_e$ oscillation probability is not sensitive to the octant degeneracy, as explained

JHEP01(2008)022

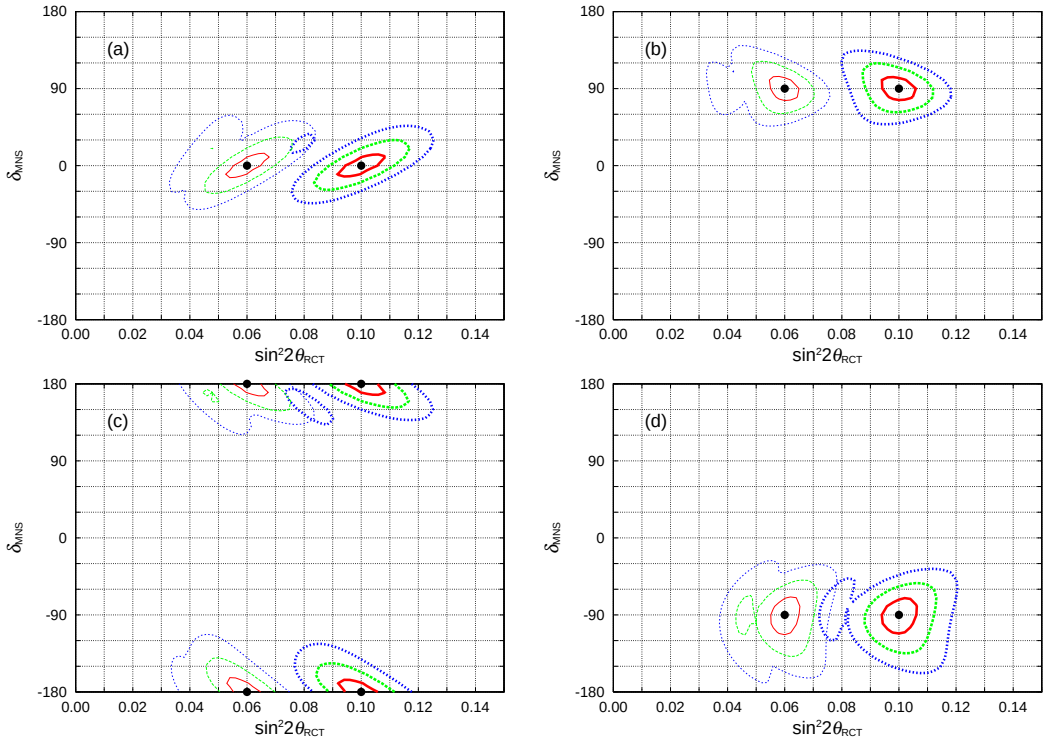

Figure 8: The allowed region in the plane of $\sin^2 2\theta_{\rm RCT}$ and $\delta_{\rm MNS}$ by the T2KK set up of figure 1, when $\sin^2\theta_{\rm ATM}^{\rm input} = 0.40$ and the hierarchy is normal. The input values of $\sin^2 2\theta_{\rm RCT}$ and $\delta_{\rm MNS}$, $\sin^2 2\theta_{\rm RCT}^{\rm input} = 0.06$ or 0.10, $\delta_{\rm MNS}^{\rm input} = 0°$ (a), 90° (b), 180° (c), and −90° (d), are denoted by solid blobs in each figure and the other input parameters are listed in eq. (4.1). The 1σ, 2σ, and 3σ contours are shown by solid, dashed, and dotted lines, respectively. The thick (thin) lines are for $\sin^2 2\theta_{\rm RCT}^{\rm input} = 0.10$ (0.06). There is no allowed region within 3σ when the inverted hierarchy is assumed with fit.

in eq. (2.14). The results we found in figure 8 confirms the validity of our approximation for the T2KK experiments.

Figure 9 also shows the potential of the T2KK experiment for measuring $\sin^2 2\theta_{\rm RCT}$ and $\delta_{\rm MNS}$, but for $\sin^2\theta_{\rm ATM}^{\rm input} = 0.60$. There is no allowed region within 3σ when the inverted hierarchy is assumed in the fit, as can be seen from figure 7(a3).

Comparing the contours of figure 9 with the corresponding ones in figure 8 of ref. [9] for $\sin^2\theta_{\rm ATM}^{\rm input} = 0.5$, we can again identify the islands due to the octant degeneracy. When $\sin^2 2\theta_{\rm RCT}^{\rm input} = 0.10$, the thick contours shows no island at $\delta_{\rm MNS}^{\rm input} = \pm 90°$, but 3σ islands appear at the other $\delta_{\rm MNS}^{\rm input}$ cases. In case of $\sin^2\theta_{\rm RCT}^{\rm input} = 0.06$, the contours have 3σ islands for all $\delta_{\rm MNS}^{\rm input}$ cases, but there is no 2σ island. These results are consistent with the result of figure 2(a). The location of the center of the islands is at around $\sin^2 2\theta_{\rm RCT}^{\rm fit} = \sin^2 2\theta_{\rm RCT}^{\rm input}$ (0.6)/(0.4), as expected by eq. (4.2). The capability of measuring $\sin^2 2\theta_{\rm RCT}$ for $\sin^2\theta_{\rm ATM}^{\rm input} = 0.60$ is also reduced by the octant degeneracy, which is the same as that for $\sin^2\theta_{\rm ATM}^{\rm input} = 0.40$. However, the octant degeneracy does not disturb the T2KK capability of determining the CP phase.

JHEP01(2008)022

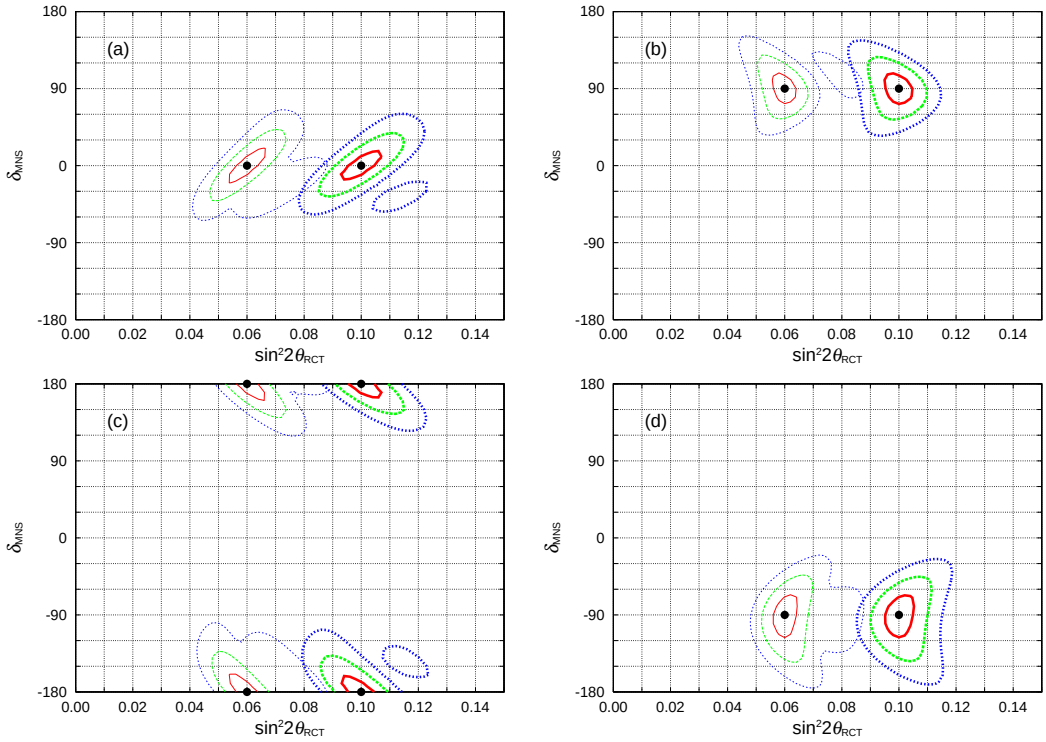

Figure 9: The same as figure 8, but for $\sin^2\theta_{\rm ATM}^{\rm input} = 0.60$.

7. Summary

There are three types of ambiguity in the neutrino parameter space. The first one is from the sign of the larger mass-squared difference, which is related to the mass hierarchy pattern. The second one is from the combination of the unmeasured parameters, the leptonic CP phase ($\delta_{\rm MNS}$) and the mixing angle $\theta_{\rm RCT}$, which resides at the upper-right corner of the MNS matrix [1]. In the previous studies [8, 9], we showed that the idea [10] of placing a 100kton-level water Čerenkov detector in Korea along the T2K neutrino beam at $L = 1000$km, the T2KK experiment [13] can solve these ambiguities. The last ambiguity is in the value of the $\theta_{\rm ATM}$, which dictates the atmospheric neutrino observation [2] and the long base-line neutrino oscillation experiment [3, 4]. If the mixing angle $\theta_{\rm ATM}$, is not 45°, there is a two fold ambiguity between "$\theta_{\rm ATM}$" and "$90^\circ - \theta_{\rm ATM}$", the octant degeneracy [16].

In this paper, we focus on the physics potential of the T2KK experiment for solving the octant degeneracy with an optimal beam combination for SK and Korean site. We follow the experimental setup found in ref. [8, 9], where SK is adopted as a near detector and 100 kton water Čerenkov detector is located at $L = 1000$km, and the J-PARC neutrino beam is observed at SK with 3.0° off-axis angle and at the far detector site in Korea with 0.5° off-axis angle.

If the value of $\sin^2 2\theta_{\rm ATM}$ is 0.99, which is 1% smaller than the maximal mixing, the value of $\sin^2\theta_{\rm ATM}$ is $\sin^2\theta_{\rm ATM} = 0.45$ or 0.55, which differ by 20%. Therefore, we also investigate the impacts of the octant degeneracy on the physics potential for the mass

JHEP01(2008)022

hierarchy determination and the CP phase measurement by T2KK, because the leading term of $\nu_\mu \to \nu_e$ oscillation probability is proportional to $\sin^2\theta_{\rm ATM}$, not $\sin^2 2\theta_{\rm ATM}$.

When we include the constraint for the value of $\sin^2\theta_{\rm RCT}$, which will be obtained from the future reactor experiments [25]. the octant degeneracy between $\sin^2\theta_{\rm ATM} = 0.40$ and 0.60 can be resolved at 3σ level for $\sin^2 2\theta_{\rm RCT} > 0.12$ (0.08) after 5 years exposure with 1.0 (5.0) $\times 10^{21}$ POT/year, if the hierarchy is normal, see figure 1 and figure 2. We find that the contribution from the second maximum of the $\nu_e \to \nu_\mu$ oscillation probability at the far detector ($L = 1000$km) plays an important role for solving the octant degeneracy. It is also found that the octant degeneracy cannot be solved without the contribution from future reactor experiments.

We also investigate the impact of the octant degeneracy in the determination of the mass hierarchy pattern. The T2KK power of resolving the mass hierarchy pattern is proportional to the value of $\sin^2\theta_{\rm ATM}^{\rm input}$ for the normal hierarchy, see figure 5, because the $\nu_\mu \to \nu_e$ rate is proportional to $\sin^2\theta_{\rm ATM}^{\rm input}$. When the mass hierarchy is normal, we can determine the mass hierarchy at 3σ level for $\sin^2 2\theta_{\rm RCT}^{\rm input} \gtrsim 0.07$ if $\sin^2\theta_{\rm ATM}^{\rm input} = 0.40$, figure 7(a1), whereas the same holds for $\sin^2 2\theta_{\rm RCT}^{\rm input} \gtrsim 0.04$ if $\sin^2\theta_{\rm ATM}^{\rm input} = 0.60$, figure 7(a3). On the other hand, if the hierarchy is inverted, $\sin^2\theta_{\rm ATM} = 0.5$ is found to be the optimal case for the mass hierarchy determination, see figure 6, because of the lower rate of the $\nu_\mu \to \nu_e$ events for $\sin^2\theta_{\rm ATM}^{\rm input} < 0.5$ and the octant degeneracy for $\sin^2\theta_{\rm ATM}^{\rm input} > 0.5$.

Finally, we check the effect of the octant degeneracy for the CP phase measurement, see figure 8 and figure 9. The CP phase can be constrained to $\pm 30^\circ$ at 1σ level for $\sin^2 2\theta_{\rm ATM} = 0.96$, even if we cannot distinguish between $\sin^2\theta_{\rm ATM} = 0.4$ or 0.6. The error does not increase from that for $\sin^2\theta_{\rm ATM} = 0.5$, because the coefficients of both sine and cosine term of $\delta_{\rm MNS}$ in the $\nu_\mu \to \nu_e$ oscillation probability are not sensitive to the octant degeneracy.

In this paper, high sensitivity to the mass hierarchy and the octant degeneracy resolution has been found because of the high energies (small off-axis angle) of the neutrino beam observed at a far detector. We should therefor expect that the background from miss-identification of NC π^0 production and CC soft-π emission events as ν_e CCQE events will be more serious than those observed at K2K. Because the possible advantage of choosing high-energy (small off-axis angle) beam at a far detector has been demonstrated clearly in this and previous papers [8, 9], dedicated studies on the influence of the background and non-Gaussian neutrino energy reconstruction at a few GeV region should be performed in the future.

Acknowledgments

We thank our colleagues Y. Hayato, A.K. Ichikawa, K. Kaneyuki, T. Kobayashi, and T. Nakaya, from whom we learn about K2K and T2K experiments. We are also grateful to K-i. Senda and T. Takeuchi for useful discussions and comments. The work is supported in part by the Core University Program of JSPS. The numerical calculations were carried out on Altix3700 BX2 at YITP in Kyoto University.

Note added

When finalizing the manuscript, we learned that a similar study has been performed by T. Kajita, et al. [28].

References

[1] Z. Maki, M. Nakagawa and S. Sakata, *Remarks on the unified model of elementary particles*, *Prog. Theor. Phys.* **28** (1962) 870.

[2] MACRO collaboration, M. Ambrosio et al., *Atmospheric neutrino oscillations from upward throughgoing muon multiple scattering in macro*, *Phys. Lett.* **B 566** (2003) 35 [hep-ex/0304037];
Soudan 2 collaboration, M.C. Sanchez et al., *Observation of atmospheric neutrino oscillations in Soudan* 2, *Phys. Rev.* **D 68** (2003) 113004 [hep-ex/0307069];
Super-Kamiokande collaboration, Y. Ashie et al., *A measurement of atmospheric neutrino oscillation parameters by Super-Kamiokande I*, *Phys. Rev.* **D 71** (2005) 112005 [hep-ex/0501064].

[3] K2K collaboration, M.H. Ahn et al., *Measurement of neutrino oscillation by the K2K experiment*, *Phys. Rev.* **D 74** (2006) 072003 [hep-ex/0606032].

[4] MINOS collaboration, P. Adamson et al., *First observations of separated atmospheric ν_μ and $\bar{\nu}_\mu$ events in the MINOS detector*, *Phys. Rev.* **D 73** (2006) 072002 [hep-ex/0512036];
MINOS collaboration, N. Tagg, *First MINOS results from the NuMI beam*, hep-ex/0605058;
MINOS collaboration, D.G. Michael et al., *Observation of muon neutrino disappearance with the MINOS detectors and the NuMI neutrino beam*, *Phys. Rev. Lett.* **97** (2006) 191801 [hep-ex/0607088].

[5] CHOOZ collaboration, M. Apollonio et al., *Search for neutrino oscillations on a long base-line at the CHOOZ nuclear power station*, *Eur. Phys. J.* **C 27** (2003) 331 [hep-ex/0301017].

[6] Homestake collaboration, B.T. Cleveland et al., *Measurement of the solar electron neutrino flux with the Homestake chlorine detector*, *Astrophys. J.* **496** (1998) 505;
SAGE collaboration, J.N. Abdurashitov et al., *Measurement of the solar neutrino capture rate by the russian-american gallium solar neutrino experiment during one half of the* 22*-year cycle of solar activity*, *J. Exp. Theor. Phys.* **95** (2002) 181 [*Zh. Eksp. Teor. Fiz.* **122** (2002) 211] [astro-ph/0204245]; *Measurement of the solar neutrino capture rate with gallium metal*, *Phys. Rev.* **C 60** (1999) 055801 [astro-ph/9907113];
GALLEX collaboration, W. Hampel et al., *GALLEX solar neutrino observations: results for GALLEX IV*, *Phys. Lett.* **B 447** (1999) 127;
Super-Kamiokande collaboration, M.B. Smy et al., *Precise measurement of the solar neutrino day/night and seasonal variation in Super-Kamiokande-I*, *Phys. Rev.* **D 69** (2004) 011104 [hep-ex/0309011];
SNO collaboration, B. Aharmim et al., *Electron energy spectra, fluxes, and day-night asymmetries of ^8B solar neutrinos from measurements with NaCl dissolved in the heavy-water detector at the Sudbury Neutrino Observatory*, *Phys. Rev.* **C 72** (2005) 055502 [nucl-ex/0502021];
GNO collaboration, M. Altmann et al., *Complete results for five years of GNO solar neutrino observations*, *Phys. Lett.* **B 616** (2005) 174 [hep-ex/0504037];

JHEP01(2008)022

SUPER-KAMIOKANDE collaboration, J. Hosaka et al., *Solar neutrino measurements in super-Kamiokande-I*, *Phys. Rev.* **D 73** (2006) 112001 [hep-ex/0508053].

[7] KAMLAND collaboration, T. Araki et al., *Measurement of neutrino oscillation with KamLAND: evidence of spectral distortion*, *Phys. Rev. Lett.* **94** (2005) 081801 [hep-ex/0406035].

[8] K. Hagiwara, N. Okamura and K.-i. Senda, *Solving the neutrino parameter degeneracy by measuring the T2K off-axis beam in Korea*, *Phys. Lett.* **B 637** (2006) 266 [*Erratum ibid.* **B 641** (2006) 491] [hep-ph/0504061].

[9] K. Hagiwara, N. Okamura and K.-i. Senda, *Physics potential of T2KK: an extension of the T2K neutrino oscillation experiment with a far detector in Korea*, *Phys. Rev.* **D 76** (2007) 093002 [hep-ph/0607255].

[10] K. Hagiwara, *Physics prospects of future neutrino oscillation experiments in asia*, *Nucl. Phys.* **137** *(Proc. Suppl.)* (2004) 84 [hep-ph/0410229];
K-i. Senda, *Solving the neutrino parameter degeneracy by measuring the T2K off-axis beam in Korea*, talk given at KEKPH2005, KEK Japan (2005)
http://research.kek.jp/group/riron/workshop/KEKPH2005/program.html.

[11] J-PARC home page, http://j-parc.jp/.

[12] THE T2K collaboration, Y. Itow et al., *The JHF-Kamioka neutrino project*, hep-ex/0106019;
JHF Neutrino Working Group's home page, http://neutrino.kek.jp/jhfnu/.

[13] *An international workshop on a far detector in Korea for the J-PARC neutrino beam*, KIAS, Seoul South Korea (2005) http://newton.kias.re.kr/~hepph/J2K/;
2*nd international workshop on a far detector in Korea for the J-PARC neutrino beam*, Seoul National Univ., Seoul South Korea (2006) http://t2kk.snu.ac.kr/.

[14] M. Ishitsuka, T. Kajita, H. Minakata and H. Nunokawa, *Resolving neutrino mass hierarchy and CP degeneracy by two identical detectors with different baselines*, *Phys. Rev.* **D 72** (2005) 033003 [hep-ph/0504026].

[15] O. Mena Requejo, S. Palomares-Ruiz and S. Pascoli, *Super-nova: a long-baseline neutrino experiment with two off-axis detectors*, *Phys. Rev.* **D 72** (2005) 053002 [hep-ph/0504015];
Determining the neutrino mass hierarchy and CP-violation in nonua with a second off-axis detector, *Phys. Rev.* **D 73** (2006) 073007 [hep-ph/0510182].

[16] M.C. Gonzalez-Garcia and C. Pena-Garay, *Global and unified analysis of solar neutrino data*, *Nucl. Phys.* **91** *(Proc. Suppl.)* (2001) 80 [hep-ph/0009041];
V. Barger, D. Marfatia and K. Whisnant, *Breaking eight-fold degeneracies in neutrino CP-violation, mixing and mass hierarchy*, *Phys. Rev.* **D 65** (2002) 073023 [hep-ph/0112119].

[17] K. Hagiwara and N. Okamura, *Quark and lepton flavor mixings in the* SU(5) *grand unification theory*, *Nucl. Phys.* **B 548** (1999) 60 [hep-ph/9811495].

[18] B. Kayser, *Review of particle physics*, *J. Phys.* **G 33** (2006) 156.

[19] L. Wolfenstein, *Neutrino oscillations in matter*, *Phys. Rev.* **D 17** (1978) 2369;
R.R. Lewis, *Coherent detector for low-energy neutrinos*, *Phys. Rev.* **D 21** (1980) 663;
V. Barger, S. Pakvasa, R.J.N. Phillips and K. Whisnant, *Matter effects on three-neutrino oscillations*, *Phys. Rev.* **D 22** (1980) 2718.

JHEP01(2008)022

[20] S.P. Mikheyev and A.Y. Smirnov, *Resonance enhancement of oscillations in matter and solar neutrino spectroscopy*, *Yad. Fiz.* **42** (1985) 1441 [*Sov. J. Nucl. Phys.* **42** (1986) 913]; *Resonant amplification of neutrino oscillations in matter and solar neutrino spectroscopy*, *Nuovo Cim.* **C9** (1986) 17.

[21] G.L. Fogli, E. Lisi, A. Marrone and G. Scioscia, *Super-Kamiokande atmospheric neutrino data, zenith distributions and three-flavor oscillations*, *Phys. Rev.* **D 59** (1999) 033001 [hep-ph/9808205];
G.L. Fogli et al., *Addendum to: solar neutrino oscillation parameters after first KamLAND results*, *Phys. Rev.* **D 69** (2004) 017301 [hep-ph/0308055].

[22] M. Koike, N. Okamura, M. Saito and T. Takeuchi, *Leptonic CP-violation search and the ambiguity of* Δm^2_{31}, *Phys. Rev.* **D 73** (2006) 053010 [hep-ph/0510082].

[23] M. Honda, Y. Kao, N. Okamura and T. Takeuchi, *A simple parameterization of matter effects on neutrino oscillations*, hep-ph/0602115.

[24] A.K. Ichikawa, private communication; The flux datas for various off-axis angles are available this web page: http://jnusrv01.kek.jp/~ichikawa/jhfnu/nubeam/655km.

[25] F. Ardellier et al., *Letter of intent for double-CHOOZ: a search for the mixing angle* θ_{13}, hep-ex/0405032;
KASKA collaboration, F. Suekane, *Status of KASKA: the japanese reactor* $\sin^2(2\theta_{13})$ *project*, hep-ex/0407016;
S.B. Kim, talk presented in *Fourth workshop on future low energy neutrino experiments*, Angra dos Reis, RJ Brazil (2005);
J. Cao, *Daya bay neutrino experiment*, *Nucl. Phys.* **155** *(Proc. Suppl.)* (2006) 229 [hep-ex/0509041].

[26] M. Furusaka, R. Hino, Y. Ikeda et al., *The joint project for high-intensity proton accelerators*, KEK-REPORT-99-4 [JAERI-TECH-99-056] [JHF-99-3].

[27] P. Zucchelli, *A novel concept for a* $\bar{\nu}/e$ *neutrino factory*, hep-ex/0107006; *A novel concept for a* $\bar{\nu}_e/\nu_e$ *neutrino factory: The beta beam*, *Phys. Lett.* **B 532** (2002) 166;
B. Autin et al., *The acceleration and storage of radioactive ions for a neutrino factory*, *J. Phys.* **G 29** (2003) 1785 [physics/0306106];
M. Mezzetto, *Physics reach of the beta beam*, *J. Phys.* **G 29** (2003) 1771 [hep-ex/0302007].

[28] T. Kajita, H. Minakata, S. Nakayama and H. Nunokawa, *Resolving eight-fold neutrino parameter degeneracy by two identical detectors with different baselines*, *Phys. Rev.* **D 75** (2007) 013006 [hep-ph/0609286].

JHEP01(2008)022